

FILE COPY  
NO. 4



TECHNICAL MEMORANDUMS  
NATIONAL ADVISORY COMMITTEE FOR AERONAUTICS

---

No. 878

---

THE TWISTING OF THIN-WALLED, STIFFENED  
CIRCULAR CYLINDERS

By E. Schapitz

Lilienthal-Gesellschaft für Luftfahrtforschung  
Jahrbuch 1936

THIS DOCUMENT ON LOAN FROM THE FILES OF  
NATIONAL ADVISORY COMMITTEE FOR AERONAUTICS  
LANGLEY AERONAUTICAL LABORATORY  
LANGLEY FIELD, HAMPTON, VIRGINIA

RETURN TO THE ABOVE ADDRESS.

REQUESTS FOR PUBLICATIONS SHOULD BE ADDRESSED  
AS FOLLOWS:

NATIONAL ADVISORY COMMITTEE FOR AERONAUTICS  
1724 F STREET, N.W.,  
WASHINGTON 25, D.C.

---

Washington  
October 1938

**FILE COPY**

To be returned to  
the files of the National  
Advisory Committee  
for Aeronautics  
Washington, D. C.



NATIONAL ADVISORY COMMITTEE FOR AERONAUTICS

TECHNICAL MEMORANDUM NO. 878

THE TWISTING OF THIN-WALLED, STIFFENED CIRCULAR CYLINDERS\*

By E. Schapitz

SUMMARY AND DEDUCTIONS

On the basis of the present investigation of the twisting of thin-walled, stiffened circular cylinders, the following conclusions can be reached:

1. There is as yet no generally applicable formula for the buckling moment of the skin. While in the DVL tests the values obtained with Donnell's formula for the buckling strength in twist of unstiffened circular cylinders are in sufficiently close agreement with the experimental results - the effects of the stiffeners and of the prebuckling canceled one another approximately - this finding cannot be looked upon as being of general validity.

2. The mathematical treatment of the condition of the shell after buckling of the skin is based upon the tension-field theory, wherein the strain condition is considered homogeneous. The strain associated with the formation of buckles is replaced by a mean contraction of the skin in circumferential direction (wrinkling  $\zeta_y$ ),

amounting, at the most, to  $\zeta_y = -\frac{\phi_1^2}{24}$  in the event that the arc length between the stringers (angle at the center  $\phi_1$ ) has shrunk to the chord length. For the stress condition it is assumed that the principal axes of stress and strain are coincident and consequently in the same direction. Assumptions are also made about the second principal stress  $\sigma_2$ . The assumptions about the wrinkling  $\zeta_y$  and the principal stress  $\sigma_2$  result in two types of tension field: namely, the complete tension field, wherein the wrinkling  $\zeta_y$  has reached the highest possible

---

\*"Über die Drillung dünnwandiger, versteifter Kreiszyklinderschalen." Lilienthal-Gesellschaft für Luftfahrtforschung Jahrbuch 1936, pp. 94-132.

value  $\zeta_y = -\frac{\varphi_1^2}{24}$  and the principal stress  $\sigma_2$  is neither locally variable nor affected by the load; and the incomplete tension field wherein  $\zeta_y < \frac{\varphi_1^2}{24}$ , and  $\sigma_2$  varies locally and is affected by the load. The treatment is extended to a case of complete tension field ( $\sigma_2 = -\tau_0$ ) and a case of incomplete tension field. For the latter, it was assumed that the stress condition midway between the stringers (with  $\sigma_2 = -\tau_0$ ) changes steadily into the condition prevailing in the skin strips over the stringers and results from the combined bending-compressive stress of the latter. From observations during tests, it was found that with increasing load the incomplete tension field "stretches" itself into a complete tension field. The functions, according to which the wrinkling and the constants of the stress condition change hereby, are, for lack of sufficient experimental data, assumed for the present.

3. The twisting tests in the DVL on stiffened circular cylinders, were accompanied by stress measurements on the skin, the stringers, and the bulkheads. In addition to that, the strains on the shell surface were recorded and the angles of twist of the shells measured. The comparison of the theoretical with the experimental results disclosed that, on assuming a complete tension field, the angles of twist were computed much too great, and the stresses in the stringers and bulkheads too high, while on assuming an incomplete tension field the theoretical results could be largely reconciled with the experimental results by suitable choice of the proper constants for the "stretching" of the tension field.

4. Applying the calculating method to the range of twisting moment at failure, the latter can be predicted sufficiently exact from buckling-bending tests on panels. For thin skin and strong stiffeners the calculation for complete tension field affords sufficiently accurate results; but if the skin is thick and the stiffeners weak, this calculation results in an underestimate of the ultimate twisting strength, hence an accurate calculation postulates an incomplete tension field.

5. Additional theoretical investigations are necessary regarding the buckling strength of the skin of stiff-

ened circular cylinders in twist, as well as on the buckling pattern originating after buckling and the related stress condition, in order to check the assumptions of the present calculations theoretically.

6. Further experiments are needed to explain the process of stretching of the sheet panels from the first formation of the buckles to the completely formed tension field. Investigations are further needed on the buckling-bending strength of stiffened sections under various load conditions for computing the ultimate torque  $P_L/Q$  of stiffened circular cylinders.

## I. INTRODUCTION

Suppose a circular cylinder with thin skin reinforced by stringers and bulkheads as in figure 1, is stressed in twist. In the following the stress distribution in the shell and the strain from the moment of applied load to final failure is investigated.

The present problem is significant for airplane statics since the circular cylinder serves as schematic substitute for the variously designed shell bodies. The latter are, in several cases, stressed simultaneously in bending with transverse force and twist. A study of the behavior of shells under combined load postulates the knowledge of the shell strength and stiffness under simple stresses. Twist is the simplest case of shearing stress; the stress from normal forces and that from bending moments have been studied previously. It may even become possible to estimate the strength of shells under combined load from simple formulas if the strength under simple loads is known. To this end a thorough investigation of the hitherto little-treated problem of twist (reference 1) is well justified.

The study is restricted to shells of very small skin thickness  $s$  in relation to the cylinder radius  $r_H$  ( $s:r < 1:400$ ); it is further assumed that at least six stringers at equal spacing  $b$  are arranged over the circumference and that the bulkheads themselves are of equal spacing  $t$ . The latter are attached to the stringers but not to the skin. The stringer section is symmetrical; the frame stiffness of the system formed by the stiffeners is disregarded.

Section II is concerned with checking the available possibilities for computing the buckling stress of the skin of a stiffened circular cylinder under twist. Section III treats the behavior of the shell after buckling of the skin, theoretically, on the basis of an improved tension-field theory, and experimentally, as reflected in twisting tests made by the DVL on stiffened circular cylinders. Section IV explores the possibility of predicting the ultimate twisting moment from the results of buckling-bending tests on shell panels.

## II. BUCKLING OF SKIN

The sheet panels between the stringers may be considered as long strips (width  $b$ ) with, originally, cylindrically curved median surface which under twist are stressed in shear. There exists up to now no theoretically founded formula for the buckling stress of such curved strips.

For the buckling stress of unstiffened circular cylinders (length  $l$ ) in shear, Donnell has developed a formula which, applied to large ratios  $r_H:s$ , reads as follows:

$$\tau_0 = 0.769 \frac{E}{(1 - \mu^2)^{5/8}} \left(\frac{s}{r_H}\right)^{5/4} \left(\frac{r_H}{l}\right)^{1/2}$$

where  $E$  is the modulus of elasticity, and  $\mu$  is Poisson's ratio. For  $\mu = 0.3$ , it is:

$$\tau_0 = 0.815 E \left(\frac{s}{r_H}\right)^{5/4} \left(\frac{r_H}{l}\right)^{1/2} \quad (1)$$

Considering the sheet sections between the stringers as flexible, built-in, shear-stressed plates, their buckling strength  $\tau_0' = 5 \frac{E}{1 - \mu^2} \left(\frac{s}{b}\right)^2$  will be of the order of magnitude of the buckling stress  $\tau_0$  computed according to equation (1), and even higher for very close stringer spacing  $b$ . It is therefore anticipated that on stiffened shells the buckling stresses  $\tau_0$ , computed according

to equation (1), will be too low. On the other hand, Donnell has indicated that the experimental values are always lower than the theoretical figures because of the pre-buckling effect.

For the shear stress in buckling of curved plate beams, H. Wagner applies the formula:

$$\tau_K = k_R E \frac{s}{r_H} + k_E E \left(\frac{s}{b}\right)^2 \quad (1a)$$

wherein  $k_R = 0.12$  and for built-in edges the value  $k_E = 9.1$ ; for superposed edges the value  $k_E = 5.3$  must be written in. The coefficients themselves are referred to an average span-chord ratio, not to a long strip.

Twisting tests made by the DVL on stiffened circular cylinders (see also under III, 2) supplied the data appended in table I. According to it, Donnell's formula yields somewhat lower values, although the agreement in view of the uncertainty surrounding the experimental solution of the buckling stress should be looked upon as being satisfactory. On the present test specimens (cylinders II, III, and IV) the prebuckling effect approximately neutralizes the stiffener effect. From this observation, no conclusions may be drawn as to shells of other dimensions - more particularly, as cylinders III and IV were already prestressed and manifested prebuckling. Wagner's formula (1a) had proved itself in tests with curved panels built in between rigid-edge members. In the present tests, it not only gives too high values but also fails to include qualitatively the difference in the buckling strength of the skin of cylinders III and IV. The explanation of this disagreement involves, other than the prebuckling effect, that of the restraint. Besides, the lengths of the earlier investigated sheet sections were much shorter compared to the skin sections on the explored shells.

The problem of buckling stress of the skin of stiffened circular cylinders in twist therefore remains largely unexplained. A thorough mathematical study is under way in the DVL.

TABLE I

Buckling Stresses and Moments of the Skin -  
Theoretical and Experimental

1	2	3	4	5	6	7	8	9	10
Cyl- inder No.	Skin thick- ness mm	Radius of shell $r_H$ mm	Angle of center $\varphi_1 = b_1/r_H$	Test figures		Theoretical values*			
				Buck- ling moment kg cm	Buck- ling stress kg/cm <sup>2</sup>	Donnell's formula		Wagner's formula**	
						Buck- ling moment kg cm	Buck- ling stress kg/cm <sup>2</sup>	Buck- ling moment kg cm	Buck- ling stress kg/cm <sup>2</sup>
II	0.4	400	0.320	31200	77.6	18600	46.3	59100	144
III	.39	400	.280	22200	56.9	18850	48.3	68200	175
IV	.54	400	.490	53400	99.0	35800	66.4	71100	132

\*With  $E = 740000 \text{ kg/cm}^2$  and  $\mu = 0.3$ .

\*\*For built-in edges with  $k_E = 9.1$ .

In the following theoretical arguments and experimental evaluations, the buckling stress is computed by formula (1).

### III. STRESS AND STRAIN AFTER BUCKLING OF THE SKIN

#### 1. Theoretical Considerations

a) Fundamental assumptions for the tension field.— Up to buckling of the skin ( $\tau < \tau_0$ ) the stress distribution is completely uniform. The principal axes of the stress slope at  $45^\circ$  toward the generating line and the principal stresses have the magnitudes  $\sigma_1 = +\tau$  and  $\sigma_2 = -\tau$ . The stringers are twisted through the same angle as the shell, whereas the bulkheads remain untouched.

Buckling of the skin is accompanied by a stress rearrangement. The ensuing skin wrinkles indicated on several exhibits of figures 2 to 4, transmit, essentially, tensile stresses in longitudinal direction, but only minor stresses in transverse direction. Through the deflection of the wrinkles the stiffener system is loaded radially

inward. Moreover, the stringers must support the shell longitudinally - that is, become stressed in compression. According to figures 2 to 4, the wrinkling can be confined to the free sheet panels between the stringers; the strips of skin riveted to the stringers do not buckle. The processes on failure are described in section IV.

In the absence of any method for solving the buckling stage of curved sheet panels in shear by means of the elasticity theory, suitable substitutes must be resorted to. In the following, the "tension field" denotes a fictitious condition, based on observations, that replaces the true stress and strain condition, and affords a comprehensive solution. The assumptions involved refer to the strain conditions and to the stress distribution.

The strain condition is considered homogeneous, and the nonuniform strain associated with the buckling is replaced by a mean circumferential contraction of the skin. This shortening of the circumference through the wrinkling (indicated hereafter as wrinkling  $\zeta_y$ ) is determined in the following manner: The traces of the median surface of the buckled skin with the longitudinal section planes placed through the axis of the shell, have wave form (fig. 5) and permit, for sufficiently great shell length, the precise determination of one mean skin radius each in each intersecting plane. The base line of the cylinder surface formed with these mean radii ("substitute surface") runs between the stringers - usually between the original arc and the chord - and is, by suitable shell length, symmetrical to the "panel center" (fig. 5). If  $b_1'$  is its arc length between stringers, and  $b_1$  the original arc length, the wrinkling  $\zeta_y$  is defined by

$$\zeta_y = \frac{b_1' - b_1}{b_1}$$
 If  $\zeta_y$  shortens the arc length to chord length, it is (with  $\varphi_1 = b_1/r_H$ )

$$\zeta_y = \frac{2r_H \sin \frac{\varphi_1}{2} - r_H \varphi_1}{r_H \varphi_1}$$

The series development of  $\varphi_1/2$ , interrupted after the term of the third degree, leaves the form  $\zeta_y = -\frac{\varphi_1^3}{24}$ .\*

\*The wrinkling was originally introduced by H. Wagner in the calculation of the angle of the principal axes.

For the stress panel it is assumed that the principal axes of stress and strain are coincident in the region between the stringers and, accordingly, in the same direction everywhere. The assumptions made about the second principal stress  $\sigma_2$  will be analyzed in section III, 1c. The skin strips above the stringers are adjudged as parts of the stringers in the width where they touch the stringers. If the sections are closed, the strip between rivet rows is counted as part of the stringers.

b) General stress and strain formulas.— Figure 6 presents a section bounded by two stringers and two bulkheads and the chosen coordinate system. From the theory of plane strain, the angle  $\alpha$  of the principal strain direction to the positive x-axis ( $\epsilon$  is the maximum positive strain) follows as:

$$\tan^2 \alpha = \frac{\epsilon - \epsilon_x}{\epsilon - \epsilon_y} \quad (2a)$$

Allowance for the assumedly homogeneous strain panel is made by the introduction of mean values for the locally variable stresses and strains in the range  $0 < x < t$  and  $-\frac{b_1}{2} < y < +\frac{b_1}{2}$ . Denoting the average value of the principal tensile stress  $\sigma_1$  with  $\bar{\sigma}_1$ , that of the compressive stress  $\sigma_x$  in the stringers with  $\bar{\sigma}_x$ , while disregarding the transverse extension due to  $\sigma_2$ , we have:

$$\epsilon = \bar{\sigma}_1 / E$$

and besides,

$$\epsilon_x = \bar{\sigma}_x / E$$

The strain  $\epsilon_y$  is composed of: the bulkhead compression  $\epsilon_{y_1} = \sigma_y / E$  ( $\sigma_y$  compressive stress in bulkhead), the wrinkling  $\zeta_y$ , and the related shortening of the shell circumference  $\epsilon_{y_2}$ , caused by the deflections  $f$  of the stringers and the local indentations  $\Delta r_H$  at their points of support at the bulkheads. Hence, we have:

$$\epsilon_{y_2} = -\frac{1}{r_H} (\bar{f} + \Delta r_H)$$

and

$$\epsilon_y = \frac{\sigma_y}{E} + \zeta_y - \frac{1}{r_H} (\bar{f} + \Delta r_H)$$

Herein  $\bar{f}$  is the average value of the deflections  $f$  between two bulkheads. Formula (2a) can be rewritten as:

$$\tan^2 \alpha = \frac{\bar{\sigma}_1 - \bar{\sigma}_2}{\bar{\sigma}_1 - \sigma_y - E \left[ \zeta_y - \frac{\bar{f} + \Delta r_H}{r_H} \right]} \quad (2b)$$

The shearing strain  $\gamma_{xy}$  follows from the strain theory as:

$$\gamma_{xy} = 2 \cot \alpha (\epsilon - \epsilon_x) = 2 \tan \alpha (\epsilon - \epsilon_y)$$

and, after insertion of equation (2a), as:

$$\gamma_{xy} = 2 \sqrt{(\epsilon - \epsilon_x) (\epsilon - \epsilon_y)} \quad (3)$$

The angle of twist of the total circular cylinder (length  $l$ ) is:

$$\psi = \gamma_{xy} \frac{l}{r_H} = \frac{2l}{r_H} \sqrt{(\epsilon - \epsilon_x) (\epsilon - \epsilon_y)} \quad (4)$$

To compute these strains the stress condition in the buckled skin must first be analyzed. The shearing stress in the section of the circular cylinder to be taken by the skin is under torque  $T$ :

$$\tau = \frac{T}{2\pi r_H^2 s} \quad (5)$$

With  $\sigma_n$  as normal stress in the section perpendicular to the generating line, and  $\sigma_r$  as the ring stress, the equilibrium equations for the skin element (fig. 7), read:

$$\sigma_1 = \sigma_n + \tau \tan \alpha$$

$$\sigma_1 = \sigma_r + \tau \cot \alpha$$

From the general formulas of the stress condition, follows:

$$\sigma_1 + \sigma_2 = \sigma_n + \sigma_r$$

so that, finally:

$$\left. \begin{aligned} \sigma_1 &= \frac{\tau}{\sin \alpha \cos \alpha} + \sigma_2 \\ \sigma_r &= \tau \tan \alpha + \sigma_2 \\ \sigma_n &= \tau \cot \alpha + \sigma_2 \end{aligned} \right\} \quad (6)$$

The angle  $\alpha$  is assumed to be known, and the four stresses  $\sigma_1$ ,  $\sigma_2$ ,  $\sigma_n$ , and  $\sigma_r$  as unknown. There being only three equations available, one of the stresses - say, the second principal stress  $\sigma_2$  - requires an assumption.

c) Special assumptions for different types of "tension field." - In the following, the assumptions from III, 1a for the tension field are supplemented by assumptions for the wrinkling  $\zeta_y$  and the second principal stress  $\sigma_2$  - and the terms "complete" and "incomplete" tension field are introduced.

By "complete" tension field is meant a stress and stress condition wherein  $\sigma_2$  is constant locally and under load, and in which the wrinkling  $\zeta_y$  corresponds to the shortening of the arc length between stiffeners to that of the chord - that is,  $\zeta_y = -\varphi_1^2/24$ . A special case of complete tension field is given by H. Wagner in his unidirectional tension field with  $\sigma_2 = 0$  and  $\zeta_y = -\varphi_1^2/24$ .

A tension field is incomplete if the principal stress  $\sigma_2$  is a function of the coordinates  $x$  and  $y$  and of the shearing stress  $\tau$ , and where the wrinkling  $\zeta_y$  has not as yet reached the value  $-\varphi_1^2/24$ .

Experiments on plate beams with flat web plates as well as the tests described under III, 2, have shown that with increasing load the condition of the incomplete tension field changes into that of the complete tension field. This process is called "stretching" of the tension field.

In the case of the complete tension field treated in the next section,  $\sigma_2$  is equated to  $-\tau_0$ , and hence it is assumed that the second principal stress prevailing when the skin buckles, preserves its magnitude even under

further strain. Then a case of incomplete tension field, suggested by the experiments, is discussed on the assumption that the principal stress  $\sigma_2$  reaches  $\sigma_2 = -\tau_0$  but only in the center of the panel between two stringers ( $y = 0$ , fig. 6), while at all other points  $\sigma_2$  remains dependent on the coordinates and the load on the basis of the following argument: The normal stress  $\sigma_n$  is (see equation 6) at  $y = 0$  for  $\sigma_2 = -\tau_0$  a tensile stress ( $\sigma_{nm}$ ), unaffected by the abscissa  $x$ , at  $y = b/2$  (see fig. 8), on the other hand (stress  $\sigma_{nL}$ ), it is governed by the combined bending-compression stress of the stringers. So, while for the complete tension field at  $y = b_1/2$ , a jump in stress (from  $\sigma_{nm}$  to  $\sigma_{nL}$ ) is assumed, for the incomplete field the change is to be uniform. For  $y = 0$ , it is:

$$\sigma_n = \sigma_{nm} = \tau \cot \alpha - \tau_0 \quad (7)$$

For the transition, it shall be:

$$\sigma_n = \sigma_{nm} - (\sigma_{nm} - \sigma_{nL}) \sin^{1/\omega} \left( \frac{\pi y}{b_1} \right) \quad (8)$$

with exponent  $1/\omega$  related to the load.

Figure 8 indicates that the curve  $\sigma_n(y)$  hugs the straight line  $\sigma_n = \sigma_{nm}$  so much closer as  $\omega$  decreases. For  $\omega = 0$  within the range of  $0 < y < b_1/2$ :  $\sigma_n = \sigma_{nm}$  and consequently, the condition of complete tension field reached. The "stretching" of the tension field taking place with increasing load is therefore bound to a decrease of  $\omega$  toward zero. For  $\omega = 0.5$ ,  $\sigma_n(y)$  is a simple sine curve. The variation of  $\sigma_2$  follows from equations (6), (7), and (8) as:

$$\sigma_2 = \sigma_n - \tau \cot \alpha = -\tau_0 (\tau \cot \alpha - \tau_0 - \sigma_{nL}) \sin^{1/\omega} \left( \frac{\pi y}{b_1} \right)$$

Since  $\sigma_{nL}$  depends on  $\tau$  and  $x$  and, in addition,  $\omega$  on  $\tau$ ,  $\sigma_2$  itself is dependent on  $x$ ,  $y$ , and  $\tau$ . For computing the stress  $\sigma_{nL}$ , the stress in the stiffeners must be analyzed.

d) The calculation of stress and strain.— The stress

in the stiffener system after buckling of the skin, consists of a radial compression due to the ring stresses, and an axial compression due to the normal stresses. The longitudinal and cross sections through the shell of figure 9 illustrate this very plainly.

The cut through the panel center between the stringers (fig. 9) must, on account of the radial symmetry, be free from shearing stresses perpendicular to the sheet surface, even for flexurally resistant sheet. In the two cases (explained under c)) of complete and incomplete tension field, the ring stress in this section is:

$$\sigma_{r_m} = \tau \tan \alpha - \tau_0 \quad (10)$$

From the equilibrium of the half shell (a) in figure 9, the bulkhead stress follows as:

$$\sigma_y F_y + \sigma_{r_m} s t = 0$$

hence,

$$\sigma_y = - \frac{s t}{F_y} (\tau \tan \alpha - \tau_0) \quad (11)$$

with  $F_y$  indicating the sectional area of the bulkheads.

In consequence of the radial symmetry of the "substitute surface," the "stretching" (Strekkenlast) load, which stresses the stringers radially as a result of the ring stress, follows as:

$$p = 2 \sigma_{r_m} s \sin \frac{\varphi}{2} \quad (12a)$$

If the angle  $\varphi$  is small enough, so that  $\sin \frac{\varphi}{2} \sim \frac{\varphi}{2}$ , then

$$p = \sigma_{r_m} s \varphi = s \varphi (\tau \tan \alpha - \tau_0) \quad (12b)$$

For incomplete tension field and curved substitute surface, a flexural sheet stiffness is presumed.

In the general case, the stringers are treated as bars supported at many points by the bulkheads; the bending moments are computed with Clapeyron's equation. With equidistant bulkhead spacing  $t$ , they are stressed like beams built in at both ends, and the bending moment is found as:

$$M_b = \frac{pt^2}{2} \left[ \frac{1}{6} - \frac{x}{t} + \frac{x^2}{t^2} \right] = \frac{1}{2} s \rho t^2 (\tau \tan \alpha - \tau_0) \left[ \frac{1}{6} - \frac{x}{t} + \frac{x^2}{t^2} \right] \quad (13)$$

The average value of this moment between two bulkheads is zero since  $\int_0^t M_b dx$  disappears as a result of the restraint tangents parallel at both ends. The deflection of the stringers is:

$$v_L = \frac{p}{E J_L} \frac{t^4}{24} \left( \frac{x^2}{t^2} - \frac{2x^3}{t^3} + \frac{x^4}{t^4} \right) \quad (14a)$$

The average is:

$$\bar{v} = \frac{p t^4}{720 E J_L} = \frac{s \rho t^4}{720 E J_L} (\tau \tan \alpha - \tau_0) \quad (14b)$$

Hereby  $J_L$  is the moment of inertia of the stringer section, including the strip of the skin assumed as being effective.  $W_L$  indicates the section modulus with respect to the neutral axis located at the skin side. The combined normal stress in the skin over the stiffener is:

$$\sigma_{nL} = \sigma_x + \frac{M_b}{W_L} \quad (15)$$

where  $\sigma_x$  is the mean compressive stress in the stringers. The average  $\bar{\sigma}_{nL}$  between two bulkheads is  $\bar{\sigma}_{nL} = \bar{\sigma}_x$ , because the mean value of  $M_b$  disappears.

No normal force being applied on the shell, the compressive stress  $\sigma_x$  in the stringers is, with allowance for the radial symmetry:

$$\sigma_x F_L + 2 s \int_0^{b_1/2} \sigma_n dy = 0$$

( $F_L$  = section of stringer) and consequently:

$$\sigma_x = - \frac{2s}{F_L} \int_0^{b_1/2} \sigma_n dy \quad (16)$$

Consider first the case of incomplete tension field and equation (8) written into equation (16). Then

$$\sigma_x = - \delta \left[ \sigma_{nm} - \frac{2}{\pi} (\sigma_{nm} - \sigma_{nL}) \int_0^{\pi/2} \sin^{1/\omega} \chi \delta \chi \right] \quad (17)$$

where  $\delta = \frac{b_1 s}{F_L}$  and  $\chi = \frac{\pi y}{b_1}$

The integral  $J(\omega) = \frac{2}{\pi} \int_0^{\pi/2} \sin^{1/\omega} \chi d\chi$  for whole num-

bered values of  $\frac{1}{\omega} = m$  divisible by 2 is obtained from:\*

$$\frac{2}{\pi} \int_0^{\pi/2} \sin^m \chi d\chi = \frac{2}{2^m} \frac{m!}{\left(\frac{m!}{2}\right)^2} \quad (18a)$$

If  $m$  is not divisible by 2, then the formula

$$\frac{2}{\pi} \int_0^{\pi/2} \sin^m \chi d\chi = \frac{2^m \left(\frac{m-1}{2}\right)!}{\pi m!} \quad (18b)$$

should be used.

Since  $\omega$  is generally fairly small ( $< 0.5$ ), that is,  $m$  great, the calculation may be limited to the whole numbered values of  $m$  and the rest interpolated. Figure 10 illustrates a curve of the integral  $J(\omega)$  for the range of  $\omega = 0$  to  $\omega = 0.5$ . Transforming equation (17) by inserting equation (15), the solution with respect to  $\sigma_x$  can be effected and yields (with  $\sigma_b(x) = M_b/W_L$ ):

\*For example, Jahnke-Emde, Funktionentafeln, 2d edition, p. 95.

$$\sigma_x = \frac{-\delta}{1 + \delta J(\omega)} \left[ \sigma_{nm} (1 - J(\omega)) + \sigma_b(x) J(\omega) \right]$$

With the abbreviation  $R = \frac{1 - J(\omega)}{1 + \delta J(\omega)}$ , this becomes:

$$\sigma_x = -\delta R \left[ \sigma_{nm} + \sigma_b(x) \frac{J(\omega)}{1 - J(\omega)} \right] \quad (19)$$

With incomplete tension field, the compressive stress  $\sigma_x$  therefore depends on abscissa  $x$  in the same manner as the bending moment. Since the mean value of  $\sigma_b(x)$  between two bulkheads disappears, the average value of  $\sigma_x$  is:

$$\bar{\sigma}_x = -\delta R \sigma_{nm} = -\delta R (\tau \cot \alpha - \tau_0) \quad (20)$$

For complete tension field  $\omega = 0$ , and hence,  $J(\omega) = 0$ ; herewith,  $R = 1$  and the compressive stress  $\sigma_x'$  becomes independent of  $x$ :

$$\sigma_x' = -\delta \sigma_{nm} = -\delta (\tau \cot \alpha - \tau_0) \quad (20a)$$

Since  $R < 1$  with incomplete tension field, the stringers are not stressed as high as with the complete field.

With complete tension field, the principal stress  $\sigma_1$  is everywhere (cf. derivation for equation 6):

$$\sigma_{1m} = \sigma_{nm} + \tau \tan \alpha \quad (21)$$

This stress prevails in the center of the panel ( $y = 0$ ) if the tension field is incomplete. Outside of the center ( $y > 0$ ), it is:

$$\sigma_1 = \sigma_n + \tau \tan \alpha = \sigma_{nm} - (\sigma_{nm} - \sigma_{nL}) \sin^{1/\omega} \left( \frac{\pi y}{b_1} \right) + \tau \tan \alpha$$

The average value of  $\sigma_1$  in the entire panel is:

$$\bar{\sigma}_1 = \frac{2}{b_1 t} \int_0^{t/2} \int_0^{b_1/2} \sigma_1 dx dy = \sigma_{nm} + \tau \tan \alpha - (\sigma_{nm} - \bar{\sigma}_x) J(\omega)$$

After inserting equation (20), we find:

$$\bar{\sigma}_1 = \tau \tan \alpha + \sigma_{nm} [1 - J(\omega) (1 + \delta R)]$$

and, since

$$1 - J(\omega) (1 + \delta R) = R$$

according to the definition of  $R$ , we have:

$$\bar{\sigma}_1 = R (\tau \cot \alpha - \tau_0) + \tau \tan \alpha \quad (22)$$

The necessary terms  $\bar{\sigma}_1$ ,  $\bar{\sigma}_x$ ,  $\sigma_y$ ,  $\bar{f}$  for computing principal axes angle  $\alpha$  follow from equations (22), (20), (11), and (14). The equation (2a) for  $\tan^2 \alpha$  is expanded with  $E/\tau_0$  or  $E/\tau$  (for unidirectional tension field)

and gives with the abbreviations  $\delta = \frac{l}{\tau_0}$ ,  $\gamma = s \frac{t}{F_y}$ , and

$$\kappa = \frac{s \varphi t^4}{720 r_H J_L} \quad \text{for incomplete and for complete tension}$$

field with  $\sigma_2 = -\tau_0$ :

$$\tan^2 \alpha = \frac{Z}{N}$$

whereby

$$Z = R (1 + \delta) (\delta \cot \alpha - 1) + \delta \tan \alpha \quad (23a)$$

and

$$N = R (\delta \cot \alpha - 1) + \delta \tan \alpha + (\gamma + \kappa) (\delta \tan \alpha - 1)$$

$$= \zeta_y \frac{E}{\tau_0} + \frac{\Delta r_H}{r_H} \frac{E}{\tau_0}$$

For complete tension field with  $\sigma_2 = -\tau_0$ , we substitute  $R = 1$  and  $\zeta_y = -\varphi_1^2/24$ . The angle of twist  $\psi$  follows from equation (4) as:

$$\psi = \frac{2l}{r_H} \frac{\tau_0}{E} \sqrt{ZN} \quad (24)$$

For the special case of unidirectional tension field ( $\sigma_2 = 0$ ), it gives:

$$\tan^2 \alpha = \frac{(1 + \delta) \cot \alpha + \tan \alpha}{\cot \alpha + \tan \alpha (1 + \gamma + \kappa) + \frac{E}{\tau} \left( \frac{\phi_1^2}{24} + \frac{\Delta r_H}{r_H} \right)} \quad (23b)$$

and the angle of twist:

$$\psi = 2 \frac{l}{r_H} \frac{\tau}{E} \times \sqrt{\left[ (1 + \delta) \cot \alpha + \tan \alpha \right] \left[ \cot \alpha + \tan \alpha (1 + \gamma + \kappa) + \frac{E}{\tau} \left( \frac{\phi_1^2}{24} + \frac{\Delta r_H}{r_H} \right) \right]} \quad (24a)$$

The total stress and strain formulas have been collected into table II.

Assuming at first the quantities  $R$ ,  $\Delta r_H$ , and  $\xi_y$  for the different loading conditions represented by  $\delta = \tau/\tau_0$  as being known, the method of computing the stress and strain in a circular cylinder in twist is as follows:

Compute the shear stress in buckling  $\tau_0$  of the skin with equation (1) or some other improved formula. The factors  $\gamma$ ,  $\kappa$ , and  $\delta$  are known construction quantities. Estimate first, angle  $\alpha$ , and check whether equation (23a) or (23b) is complied with. If such is not the case, try an angle  $\alpha$  greater or smaller as the right-hand side of the equation became too great or too small. The method converges quite rapidly. Together with the function  $\alpha(\delta)$ , compute the angle of twist according to equation (24) or (24a). Having ascertained these functions, the stresses and strains then follow from the formulas of table II.

e) Provisional assumptions on the "stretching" of the tension field.— The calculation derived in the preceding section is feasible only when  $\xi_y(\delta)$  and  $R(\delta)$  or  $\omega(\delta)$  are known. Both functions should largely be dependent upon the two parameters  $s/r_H$  and  $\phi_1 = b_1/r_H$  only, since mechanical similitude is to be assumed. Their exact solution demands exhaustive experiments.

The functions  $\xi_y(\delta)$  and  $R(\delta)$  can be ascertained, for example, by exact bulkhead stress  $\sigma_y$  measurement on a stiffened shell and determination of the angle  $\alpha$  from

the test data with the aid of equation (11). If this is supplemented by a record of the mean compressive stress

$\sigma_x$  in the stringers at point  $\frac{x}{t} = \frac{1}{2} + \frac{\sqrt{3}}{6}$  ( $M_b = 0$ ), then  $R(\delta)$  can be determined from equation (20). The angle of twist  $\psi$  must be obtained from experimental data; from equations (24) and (23a), we have (for  $\Delta r_H = 0$ ):

$$\zeta_y = \frac{\tau_0}{E} [R (\delta \cot \alpha - 1) + \delta \tan \alpha + (\gamma + \kappa) (\delta \tan \alpha - 1)] - \frac{\psi^2 r_H^2 E}{4\tau_0^2 [R (1 + \delta) (\delta \cot \alpha - 1) + \delta \tan \alpha]} \quad (25)$$

Equation (23a) for  $\tan^2 \alpha$  may serve as check.

For evaluating the experiments described in section III, 2, some provisional assumptions for the functions  $\zeta_y(\delta)$  and  $R(\delta)$  were introduced. For  $\zeta_y$ , we assumed:

$$\zeta_y = - \frac{\varphi_1^2}{24} \sqrt{\frac{\delta - 1}{\delta_z - 1}} \quad (26)$$

the incomplete changing to complete tension field, if  $\delta = \tau/\tau_0$  has reached the value  $\delta_z$  introduced as free value.

For the variation of the reduction factor  $R$ , a linear relationship was assumed in the experimental range, whereby a value  $R_0$  extrapolated with respect to  $\delta = 1$  enters as second free value. The assumed relation reads:

$$R = R_0 + (1 - R_0) \frac{\delta - 1}{\delta_z - 1} \quad (27)$$

The proper selection of  $R_0$  and  $\delta_z$  and the extent of approval of the assumed relations in comparison with the measurements will be discussed in the next section.

f) Comparison with earlier calculation methods.— The calculation methods deduced earlier by Ebner and Heck (reference 1), and Wagner and Ballerstedt (reference 2), for the stiffened circular cylinder and the plate girder with curved web plate, respectively, are predicated on the assumption of complete, unidirectional tension field, sudden appearance  $\zeta_y$  with buckling, and subsequent independence ( $\zeta_y = -\varphi^2/24$ ) from further load. Participation of skin

strip above the stringers is omitted. The skin buckling strength is allowed for by substituting the excess  $\tau - \tau_0$  for the shearing stress  $\tau$  in all equations.\* The pure shearing condition at the instant of buckling is visualized as being superposed on the unidirectional stress condition of the tension field. Since the two conditions do not have the same principal axes, the direction of the principal strain is coincident with that of the principal stress of the tension field but not with that of the principal stress resulting from the superposition. The formulas for the Ebner-Heck method are shown in table II; the calculation (see section III, 2) was checked on the experimental data.

## 2. Twisting Tests with Stiffened Circular Cylinders

a) Procedure and interpretation of tests.— The circular cylinders used by the DVL for these twist tests are shown in figure 11. The principal dimensions are given in table III. Cylinders III and IV had been subjected to prestresses as a result of other kinds of tests prior to the stress measurements and the ultimate twist tests.

The loading arrangement for applying pure torque is shown in figure 12. The length changes were recorded on Huggenberger and Okhuizen-Staeger type strain gages attached to the test specimens by spiral springs. The determination of the stresses from the length changes proceeded on the basis of modulus of elasticity of  $E = 740,000 \text{ kg/cm}^2$ .

Since the violent vibrations accompanying the formation of buckling precluded an accurate tensiometer reading during the buckling process, the strain changes had to be measured at a pre-load located considerably above the buckling load. The stages of the torque within which the stress changes were recorded, ranged at:

133,500 kg/cm and 178,100 kg/cm on cylinder No. II

71,300 kg/cm and 133,500 kg/cm on cylinders Nos. III and IV

Between these load stages the changes of the following stresses were recorded:

---

\*Wagner and Ballorstedt remove the principal stress  $\sigma_1$ , resulting in uncertainty in vicinity of buckling as pointed out by the authors.

1. The principal tensile stress ("tension diagonal stress")  $\sigma_1$ .
2. The compressive stress  $\sigma_x$  in the stringers.
3. Compressive stress  $\sigma_y$  in the bulkheads.
4. Bending stress  $\sigma_b$  in the stringers.

TABLE III

## Dimensions of Test Specimens

Cylinder No.	Skin thickness mm	Sections			Proportion of stringers to total section percent	Number of stringers	Bulkhead spacing cm	Length $l$ between clamping rings mm	Remarks
		Stringer cm <sup>2</sup>	Skin cm <sup>2</sup>	Total cm <sup>2</sup>					
II	0.4	18X0.432 = 0.77	10.50	18.27	42.6	18	36	2200	
III	.39	8.72	10.04	18.76	46.5	18	36	1840	
IV	.54	6.25	13.95	22.20	31.0	12	36	2200 1840	Stress-strain Breaking test

Figure 13 indicates the test stations. The tension-diagonal stresses were measured at a median line of the panel between two stringers; that is, at the lowest and highest points and at the turning points of the wrinkles, while the tensiometers were mounted with the gage length in the direction of the wrinkles. The stresses were measured at the stringer sections and on the skin strips over them, and - with a view to checking the relationships  $\sigma_x(x)$  and  $\sigma_b(x)$  - at five points each in three panels between the bulkheads.

The angles of twist of the shells were measured across the entire strain range up to failure. The elastic lines of the stringers and the form of wrinkles were recorded in the range of the load stages cited above. The angles of

twist were recorded with plumb lines attached to the clamping ring and to the loading ring. The strains on the cylinder surface were recorded on a mechanical bridge (fig. 14) constructed by Engineer Freitag. It carries 18 dial gages capable of registering radial displacements of the surface points along a generating line of the shell. This made it possible to record on a stringer the elastic lines under different loads as well as to determine the shifting of the support points on the bulkheads. For recording the form of the wrinkles, the bridge was started at zero load and at the load stages mentioned above on two sheet panels along every three equidistant generating lines. The surface measurements were confined to cylinders III and IV.

The bending moment  $M_b$  and the mean compressive stress  $\sigma_x$  in the stringers should be computed from the stresses  $\sigma_I$  and  $\sigma_{III}$  (fig. 13), according to the following formulas:

$$M_b = \frac{(\sigma_{III} - \sigma_I) J_L}{|e_{III}| + |e_I|} \quad (28)$$

$$\sigma_x = \frac{\sigma_{III} |e_I| + \sigma_I |e_{III}|}{|e_{III}| + |e_I|} \quad (29)$$

Entering the compressive stresses as positive, the bending moments effecting tensile stresses on the skin side of the sections will be positive. The distances  $e_I$  and  $e_{III}$  belonging to test stations I and III from the section centroid are written in with their amounts. On account of  $J_L$ ,  $e_I$ , and  $e_{III}$ , the position of the points computed, according to equations (28) and (29), depends upon the assumption of effective skin strip. These "experimental values" of  $M_b$  and  $\sigma_x$  can therefore be compared only with such theoretical values as are computed on the basis of the same assumption.

For the comparison of the theory and the experiments, it was assumed that the local indentations  $\Delta r_H$  undergone by the bulkheads at the points of support of the stringers, are proportional to the transverse load  $p$  throughout the range from incipient buckling ( $\tau = \tau_0$ ) to the end of the previously cited test range. The factor of rise is obtained from comparing the recorded indentations at start and end of the range and the related transverse loads.

For the range from end of test range to failure, the factor of rise was figured at half as great as in the test range for the purpose of allowing for the fact that, due to the effect of the webs, the bulkheads become increasingly harder against growing local indentations. The indentations may be seen in figures 24 and 25.

The cylinders Nos. III and IV were computed on the basis of the complete and of the incomplete tension field, according to the method described in section III, 1, while the method of Ebner-Heck was checked also. For the incomplete tension field the free values  $R_0$  and  $\delta_z$  were so chosen that the discrepancies of the theoretical from the experimental figures at the angles of twist and failing strengths (explained in section IV) became minimum. The figures are appended in table IV.

b) Shell stresses.— All stress changes treated in the following, relate to the stages of torque cited under III, 1a. The changes in the principal tensile stress  $\sigma_{1m}$  obtained for the panel center between stringers, are plotted against  $x$  in figure 15; the section of the wrinkles is indicated below it. The test values on cylinder III (thin skin, many wrinkles) are substantially the same at the various points of the wrinkles, whereas at the highest and lowest points of the wrinkles on cylinder No. IV, they are maximum and disclose minimum values at the turning points. On cylinder No. III, the test values are considerably scattered around a mean value approximately constant over the length. The theoretical values, constant over  $x$ , according to all methods, lie on the average in the center of the scattered experimental values, thus confirming the aspect of a complete tension field in the center of the panel.

The bending moments  $M_p$  (fig. 16), computed from the test data with the aid of equation (28), follow over  $x$ , according to a kind of bending moment line for uniformly distributed load and two-end restraint. The curves for both the complete and incomplete tension field are coincident and yield excessive values for cylinder III. For cylinder IV, the agreement is better although a few experimental values diverge in the vicinity of  $x = t$ .

As regards the compressive stresses  $\sigma_x$  in the stringers (fig. 17), the test values in the center between bulkheads are lower than at the bulkhead points  $x = 0$  and  $x = t$ . On cylinder No. III, the curve computed for incomplete tension field runs through the scatter range of

the experimental values; on cylinder No. IV, it corresponds to that of the test points but the stresses are computed about 50 percent too high. With the assumption of complete tension field, the calculation disregards the variation of  $\sigma_x$  with  $x$ ; the values themselves are substantially too high, especially on cylinder No. IV, and by the Ebner-Heck method, the divergence is even greater.

The test data on the bulkhead stresses  $\sigma_y$  (fig. 18), are misleading at the points of support of the stringers on cylinder No. III, as a result of local deflection of the flanges; hence, the averaging must be done with the values at the points between the stringers. The theoretical values for complete and incomplete tension field are coincident again; they are about 25 percent too high on cylinder No. III, and border the scatter zone of the experimental points on cylinder No. IV. By the Ebner-Heck method, the error is still greater.

c) Strain.— From the buckling pattern of the skin in figures 2 to 4, it may be seen that the wave length of the wrinkles increases with increasing width of the panels between stringers. The wave length and position of the wrinkles are not substantially altered during the strain, although the wrinkles become deeper and the points of deflection at the stringers are plainly discernible. The "angle of wrinkling" formed by the generating lines of the approximately prismatic wrinkles in the center between the stringers with the generating lines of the circular cylinder remains largely constant under increasing twist. Figure 19 presents various cross sections of the buckling pattern for cylinders III and IV. The median curve of these sections which is the base line of the "substitute surface" mentioned in section III, 1a, lies on cylinder No. III, near to the chord, on cylinder No. IV, between the original circular arc and the chord.

The plotting of the observed angles of twist, recomputed to original free length of 220 centimeters (fig. 20), indicates that cylinder No. II has lowest rigidity with respect to twist, while No. III has the greatest twisting rigidity; cylinder No. IV manifested, under first loading, a sudden rise in angle of twist on buckling, which was not observed when the load was repeated.

Figure 21 shows the computed angle  $\alpha$  of the principal axes' directions against the torque. For incomplete tension field, angle  $\alpha$  on buckling of  $45^\circ$  decreases with

vertical tangent, passes through a minimum, and slowly increases again. For complete tension field, the angle  $\alpha$  jumps at  $\tau = \tau_0$  to an angle  $\alpha_0$  dependent on the structural quantities and the buckling stress  $\tau_0$ , and rises evenly. In both cases the angles would, at very high values of  $T/T_0$  approach one and the same value, affected only by  $\gamma$ ,  $\kappa$ , and  $\delta$ , provided no change in material behavior occurred in the meantime. The computed principal axes' angles do not agree with the measured angles of wrinkles. In principle elastic displacements in the directions inclined under the angle of wrinkling are definitely feasible. By the Ebner-Heck method, angle  $\alpha$  jumps from  $45^\circ$  to  $0^\circ$  when  $T = T_0$ , only to rise again immediately with vertical tangent, and then follow a course similar to that for complete tension field.

In the solution of the angles of twist (fig. 20), on the assumption of incomplete tension field, the correct choice of  $R_0$  and  $\delta_z$  affords a satisfactory agreement between the computed curve  $\psi(T)$  and the test points. The theoretical values are somewhat too high on cylinder No. III, but a more favorable choice of  $R_0$  and  $\delta_z$  would result in an excessively high theoretical failing strength. (Cf. section IV.) For  $\tau = \tau_0$ , the calculation involves a minor jump in angle of twist, since the share of  $\epsilon$  in equations (2a) and (4), due to the second principal stress  $\sigma_2$  and the radial displacement, is not allowed for. Assuming a complete tension field, the sudden wrinkling ( $\gamma$  at  $T = T_0$ , results in a great jump of angle of twist; the computed values are much too high throughout the entire range. By the Ebner-Heck method, it gives  $\psi = 0$  and  $\frac{d\psi}{dT} = \infty$  at  $\tau = \tau_0$ ; in the further course the computed angles of twist themselves are too great, although the error is somewhat less than with the complete tension-field method.

d) Review of the calculating methods. - Under the assumption of incomplete tension field, the calculation for cylinders Nos. III and IV can, by proper selection of  $R_0$  and  $\delta_z$  be brought into satisfactory agreement with the experimental results, both as regards buckling stiffness and ultimate buckling strength (fig. 20, and section IV). The provisional assumptions, equations (26) and (27), are therefore practical to a certain extent for defining the "stretching" of the sheet panels. With the chosen  $R_0$  and  $\delta_z$ , the compressive stresses  $\sigma_x$  of the stringers

on cylinder No. III are correct within the experimental range, but too high for cylinder No. IV. The latter is probably due to the stronger than linear decrease of curve  $R(\delta)$  against  $\delta = \frac{\tau}{\tau_0} = 1$ . The ring stresses on cylinder IV are obviously computed correctly since the theoretical and experimental values for bending moments and bulkhead stresses are approximately the same. The theoretical values for bending moment and bulkhead stresses are too high for cylinder No. III. A plausible explanation for this is that the second principal stress, even in the center, between stringers, is somewhat dependent on the shearing stress  $\tau$ . But a complete explanation is impossible until the legitimacy of  $R(\delta)$  and  $\zeta_y(\delta)$  has been proved by experiments.

With the use of the complete tension field, the angles of twist are much too high. This divergence is largely attributable to the assumption of wrinkling  $\zeta_y$  on buckling. The compressive stresses in the stringers are tolerably correct within the experimental range for cylinder No. III, since  $R \sim 1$ ; but the fact that  $R < 1$  results in markedly excessive theoretical values for  $\sigma_x$  on cylinder No. IV. As to bulkhead stresses and bending moments, the same statement made for incomplete tension field holds true.

With the compressive stresses in the stiffeners as a result of the omitted effective skin strip and (on cylinder No. IV, especially) the different kind of allowance for the skin-buckling strength, the Ebner-Heck method yields even greater errors than the calculation for complete tension field; and the results are similar with the Wagner-Ballerstedt method.

The solution of the twisting stiffness is therefore contingent upon accurate experiments on the behavior of the sheet panels in the buckling stage; for this, account of the "incomplete tension field" is absolutely essential. On the contrary, calculation on the basis of complete tension field is practical for estimating the expected stresses, since it comprises their order of magnitude and always remains on the safe side.

TABLE IV

Comparison of Theoretical and Experimental Failing Torque Values

Cyl- inder No.	Experi- mental failing torque  $T_B$ kg cm	Theoretical failing torque and discrepancies					
		Complete tension field		Incomplete tension field			
		Theoret- ical failing moment kg cm	Discrep- ancy  percent	Free value  $R_0$	$\delta_z$	Theoret- ical failing moment kg cm	Discrep- ancy  percent
II	198,500	-	-	-	-	-	-
III	307,000	309,800	+1.0	0.85	43	318,200	+3.8
IV	231,000	198,200	-16.2	.72	60	250,000	+8.1

## IV. INVESTIGATION OF THE FAILING TORQUE

## 1. The Failing Torque and Its Solution

The failing torque is, according to table IV, highest on cylinder No. III; lowest on cylinder No. II. In all cases the failure takes place as column effect of the stringers. On cylinder No. II (figs. 22 and 23), the stringers are twisted, as a result of which the effective moment of inertia of the sections continues to drop as the load increases. Cylinder No. III (fig. 24), being of closed profile form, does not manifest this phenomenon; failure takes place as the result of denting of the section flanges. The webs of the open-hat sections of cylinder No. IV (fig. 25), twist individually, while the back of the section is dented in. The strips of the sheets riveted to the sections are dented on the very points of failure as a result of the buckling of the sections; on the remaining points they remain smooth. This fact permits the application of the assumption of effective sheet to the solution of the ultimate torque.

It is logical to compute the ultimate torque on the basis of buckling-bending tests with shell panels. In the following the bulkheads are assumed to be strong enough to effect a buckling of the stringers in one wave each in every bulkhead panel.

The compression in a stringer is  $P_L = \bar{\sigma}_x F_L$ ; the static cross load on it between two bulkheads is  $Q = p t$ . The ratio  $\lambda = P_L/Q$  between both follows from equations (12b) and (20) as:

$$\lambda = - \frac{b_1}{\varphi t} R \frac{\delta \cot \alpha - 1}{\delta \tan \alpha - 1} \quad \text{with} \quad \delta = \frac{\tau}{\tau_0} \quad (30)$$

Shells with thin skin and strong stiffeners may be expressed with  $\lambda \sim - \frac{b_1}{\varphi t} R \cot^2 \alpha$  when approaching failure. The ratio  $\lambda$  therefore depends upon  $\delta$ ; this function  $\lambda(\delta)$  can be computed if  $\alpha(\delta)$  and  $R(\delta)$  are known. The axial load on each stiffener is:

$$P_L = - \delta R F_L \tau_0 (\delta \cot \alpha - 1) \quad (31)$$

In the buckling-bending tests the shell panels, being of a length equal to the bulkhead spacing, are subjected to a uniformly distributed cross load. The ends of the sections should be built in. Figure 26 indicates the loading and the experimental arrangement. The ratio  $\lambda = P_L/Q$  is varied during the tests; the failing loads  $P_{LB}$  are plotted against  $\lambda$ , figure 27. Given the relation  $P_{LB}(\lambda)$  and the function  $\lambda(\delta)$  (fig. 28), a function  $P_{LB}(\delta)$  is obtainable that gives the axial loads still supported under the different stress conditions  $\delta$  on the basis of the related load conditions  $\lambda$ . The intersection of the curves  $P_L(\delta)$  and  $P_{LB}(\delta)$  defines the stress condition  $\delta_B$ , at which the shell should fail as a result of exhausted carrying capacity of the longitudinal sections. The ultimate torque is  $T_B = \delta_B T_0$ . The argument holds only for the case that the axial load  $P_L$  remains below the Euler buckling load for supported bar ends.

## 2. The Buckling-Bending Tests on Shell Panels

The shell panels consisted of two longitudinal sections bordering a riveted skin panel, and resembled a sheet panel of the respective cylinder. The length of the panels equaled the bulkhead spacing of the cylinder. The skin section was not fastened to the clamping angles and was not subject to any outside compression. The cross load (fig. 26) was distributed as evenly as possible over the length by means of wooden strips and felt liners.

The test procedure and the aspect of the break were the same as for the cylinder test. The sections of the panels belonging to cylinder No. III, failed after indentation of the flanges; but those of panel 13a (cylinder IV) failed through twisting failure of the webs.

The tests indicated (fig. 27) on the panels with closed sections (of cylinder III), first a rapid, and subsequently a slower, increase in the failing load  $P_{LB}$  with the load ratio  $\lambda = P_L/Q$ . For the panels with open sections (cylinder IV), the ultimate axial load within the explored range ( $\lambda$  between 3 and 4) is very little affected by  $\lambda$ . All experiments indicate a wide scatter zone. For the solution of the twisting stiffness the lower margin of this zone is decisive, since the failure is always initiated by the weakest of a large number of identically stressed sheet panels.

Loading two individual stiffeners instead of a panel, the former - if of closed section - proved stronger than the sheet panels in spite of the absence of the skin section, because with the latter the buckling of the section flanges is initiated by the skin. On the panels of open sections the skin had no effect on the strength.

### 3. Checking the Calculation against the Test Data

The calculation of the breaking torque included both the complete and the incomplete tension field. The data appended in table IV allows a comparison with the experimental results.

Premised on a complete tension field, the breaking torque of cylinder No. III was computed exact at 1.5 percent, while on cylinder No. IV, it was computed 16.2 percent too low. From this it follows that with thin skin and strong stiffeners the assumption of incomplete tension field leads to a sufficiently exact solution of the strength. For somewhat thicker skin and weaker stiffeners, the values by this calculation method are too low, since the tension field even at failure is still not completely stretched.

The calculating method for incomplete tension field contains the free values  $R_0$  and  $\delta_z$  which on cylinder No. IV could be so chosen that the theoretical and experi-

mental angles of twist would give the same results. With these free values, the breaking torque is computed 8.1 percent too high; this discrepancy is of the order of magnitude of the scatter in the buckling-bending tests. On cylinder No. III, the values  $R_0$  and  $\delta_z$  were so chosen that the discrepancy remained small for the angle of twist as well as for the breaking torque. With a value  $R_0 = 0.74$ , the theoretical and experimental values of the angle of twist are identical, while the theoretical breaking torque is about 25 percent too high.

It should be remembered that the buckling-bending test with sheet panels does not completely reproduce the effect of the wrinkling deflections at the stringers, because the wrinkles - in contrast to the transverse load applied in panel tests - twist the section flange and so initiate its buckling.

Translation by J. Vanier,  
National Advisory Committee  
for Aeronautics.

#### REFERENCES

1. Heck, O. S., and Ebner, Hans: Methods and Formulas for Calculating the Strength of Plate and Shell Constructions as Used in Airplane Design. T.M. No. 785, N.A.C.A., 1936.
2. Wagner, H., and Ballerstedt, W.: Tension Fields in Originally Curved, Thin Sheets During Shearing Stresses. T.M. No. 774, N.A.C.A., 1935.

**Table II.**  
Formulas for computing  
the twist of thin-  
walled, stiffened,  
circular cylinders.

Stress/Strain	Complete	Based on Incomplete Tension field	Calculated according to Ebner and Heck
Shearing stress		$\tau = \frac{T}{2\pi r_H^2 s} = \theta \cdot \tau_0$	
Donnell's shear stress in buckling		$\tau_0 = 0.815 E \left(\frac{s}{r_H}\right)^{1/2} \cdot \left(\frac{r_H}{l}\right)^{1/2}$	
Bulkhead stress $\sigma_y$	$\sigma_y = -\frac{s \cdot t}{F_y} \tau_0 (\theta \operatorname{ctg} \alpha - 1)$		$\sigma_y = -\frac{s t}{F_y} \tau_0 \operatorname{tg} \alpha (\theta - 1)$
Stringer load $p$	$p = s \varphi \tau_0 (\theta \operatorname{tg} \alpha - 1)$		$p = s \varphi \tau_0 \operatorname{tg} \alpha (\theta - 1)$
Bending stress of stringers $\sigma_b(x)$	$\sigma_b(x) = \frac{s \varphi t^2}{2 W_L} \tau_0 (\theta \operatorname{tg} \alpha - 1) \left(\frac{1}{6} - \frac{x}{t} + \frac{x^2}{t^2}\right)$		$\sigma_b(x) = \frac{s \varphi t^2}{2 W_L} \tau_0 \operatorname{tg} \alpha (\theta - 1) \left(\frac{1}{6} - \frac{x}{t} + \frac{x^2}{t^2}\right)$
Deflection of stringers (average)		$\bar{f} = \frac{s \varphi t^4}{720 E J_L} \tau_0 (\theta \operatorname{tg} \alpha - 1)$	$\bar{f} = \frac{s \varphi t^4}{720 E J_L} \tau_0 \operatorname{tg} \alpha (\theta - 1)$
Normal stress $\sigma_n$	$\sigma_n = \tau_0 (\theta \operatorname{ctg} \alpha - 1)$	$\sigma_n = \tau_0 (\theta \operatorname{ctg} \alpha - 1) \left[1 - \sin^{1/\omega} \left(\frac{\pi y}{b_1}\right) (1 + \delta R)\right] - \sigma_b(x) \frac{\delta}{1 + \delta} (1 - R) \sin^{1/\omega} \left(\frac{\pi y}{b_1}\right)$	$\sigma_n = \tau_0 \operatorname{ctg} \alpha (\theta - 1)$
Principal stress $\sigma_1$	$\sigma_1 = \tau_0 \left(\frac{\theta}{\sin \alpha \cos \alpha} - 1\right)$	$\sigma_1 = \sigma_n + \tau \operatorname{tg} \alpha$	$\sigma_1 = \tau_0 \frac{(\theta - 1)}{\sin \alpha \cos \alpha}$
Principal stress $\sigma_2$	$\sigma_2 = -\tau_0$	$\sigma_2 = \sigma_n - \tau \operatorname{ctg} \alpha$	In superposed tension field : $\sigma_2 = 0$
Compressive stress in stringers $\sigma_x$	$\sigma_x = -\delta \tau_0 (\theta \operatorname{ctg} \alpha - 1)$	$\sigma_x = -\delta R \tau_0 (\theta \operatorname{ctg} \alpha - 1) - \frac{\delta}{1 + \delta} (1 - R) \sigma_b(x)$	$\sigma_x = -\delta \tau_0 \operatorname{ctg} \alpha (\theta - 1)$
Load ratio $\lambda = P_L/Q$	$\lambda = -\frac{b_1}{\varphi \cdot t} \frac{\theta \operatorname{ctg} \alpha - 1}{\theta \operatorname{tg} \alpha - 1}$	$\lambda = -\frac{b_1}{\varphi \cdot t} R \frac{\theta \operatorname{ctg} \alpha - 1}{\theta \operatorname{tg} \alpha - 1}$	$\lambda = -\frac{b_1}{\varphi \cdot t} \cdot \operatorname{ctg}^2 \alpha$
Angle $\alpha$ of principal axes $\operatorname{tg}^2 \alpha = Z/N$	$Z = (1 + \delta) (\theta \operatorname{ctg} \alpha - 1) + \theta \operatorname{tg} \alpha$ $N = \theta (\operatorname{ctg} \alpha + \operatorname{tg} \alpha) - 1 + (\gamma + \varkappa) (\theta \operatorname{tg} \alpha - 1) + \frac{E}{\tau_0} \left(\frac{\varphi_1^2}{24} + \frac{\Delta r_H}{r_H}\right)$	$Z = R (1 + \delta) (\theta \operatorname{ctg} \alpha - 1) + \theta \operatorname{tg} \alpha$ $N = R (\theta \operatorname{ctg} \alpha - 1) + \theta \operatorname{tg} \alpha + (\gamma + \varkappa) (\theta \operatorname{tg} \alpha - 1) - E/\tau_0 (\varepsilon_v - \Delta r_H/r_H)$	$Z = (\theta - 1) (\operatorname{tg} \alpha + \operatorname{ctg} \alpha (1 + \delta))$ $N = (\theta - 1) (\operatorname{ctg} \alpha + \operatorname{tg} \alpha (1 + \gamma + \varkappa)) + E/\tau_0 (\varphi_1^2/24 + \Delta r_H/r_H)$
Angle of twist $\psi$		$\psi = 2 l/r_H \cdot \tau_0/E \sqrt{Z \cdot N}$	

Abbreviations:  $\chi = \frac{\pi y}{b_1}$       $J(\omega) = \frac{2}{\pi} \int_0^{\frac{\pi}{2}} \sin^{1/\omega} \chi d\chi$       $R = \frac{1 - J(\omega)}{1 + \delta J(\omega)}$       $\delta = \frac{b_1 \cdot s}{F_L}$       $\gamma = \frac{s \cdot t}{F_y}$       $\varkappa = \frac{s \varphi t^4}{720 r_H \cdot J_L}$

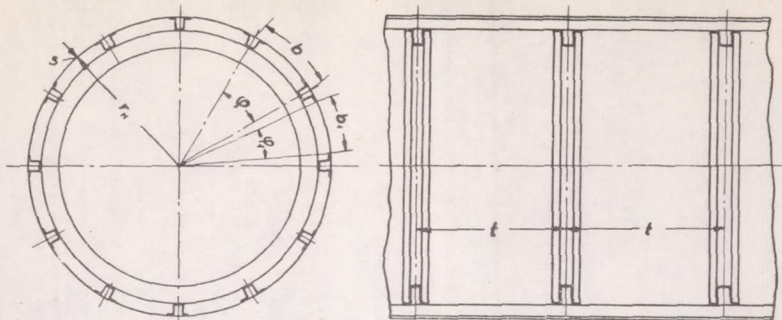


Figure 1.- Sketch of a stiffened circular cylinder.

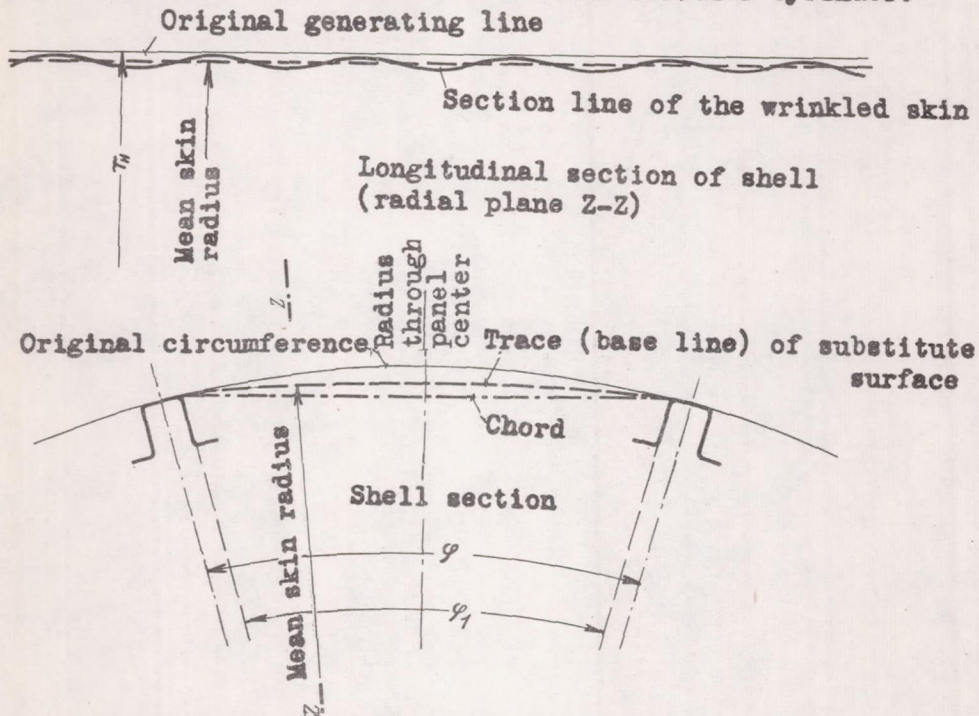


Figure 5.- Determination of wrinkling  $\{\gamma\}$ .

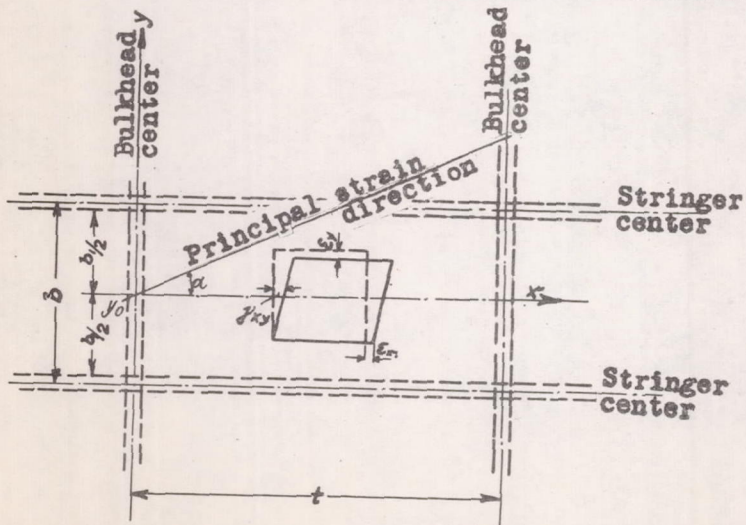


Figure 6.- Coordinate system and strain components.

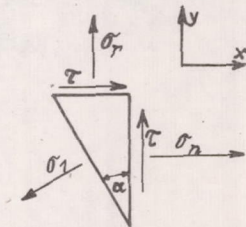


Figure 7.- Equilibrium at skin element

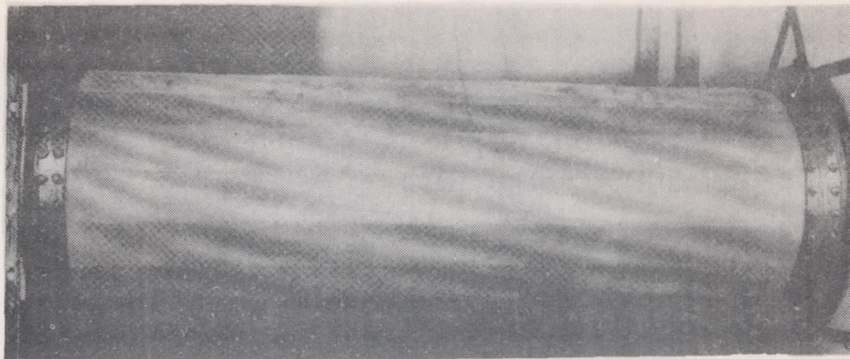


Figure 2.- Cylinder No. II after buckling of the skin.



Figure 3.- Cylinder No. III after buckling of the skin.



Figure 4.- Cylinder No. IV after buckling of the skin.

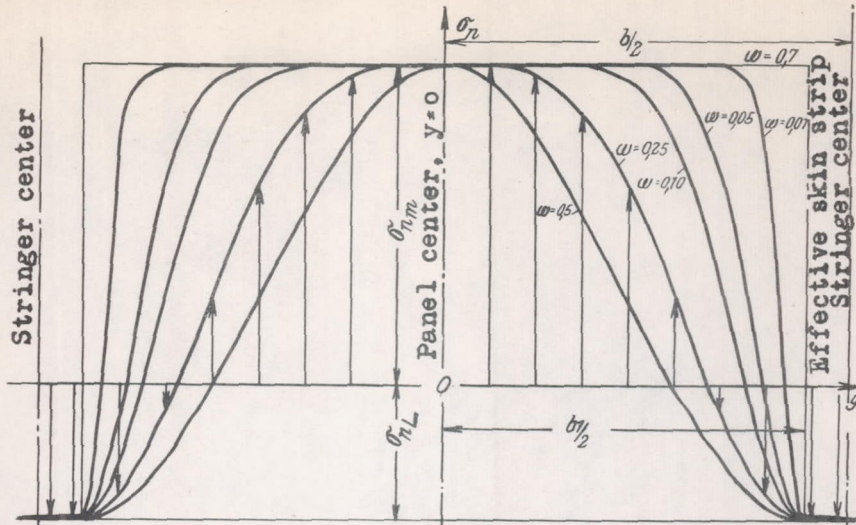


Figure 8.- Normal stress distribution  $\sigma_n$  across panel width.

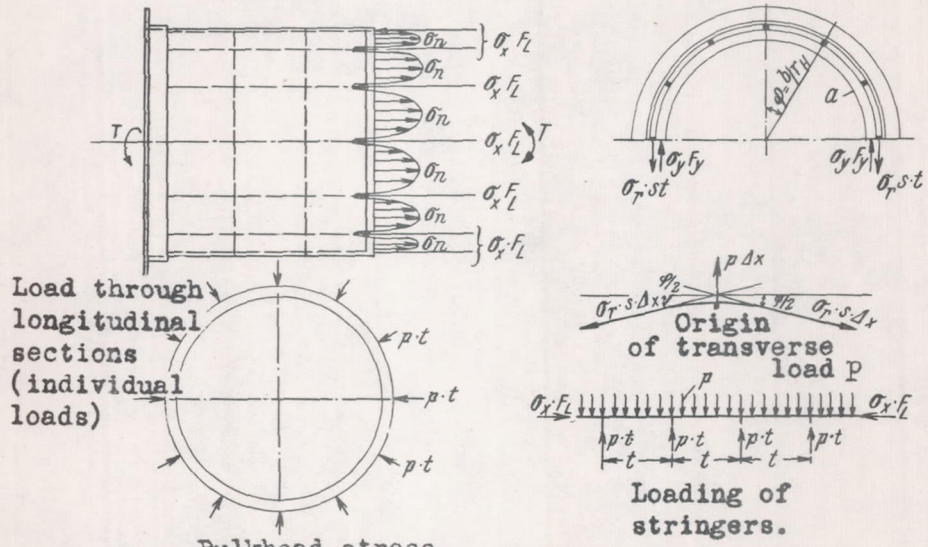


Figure 9.- Loading of stiffener system.

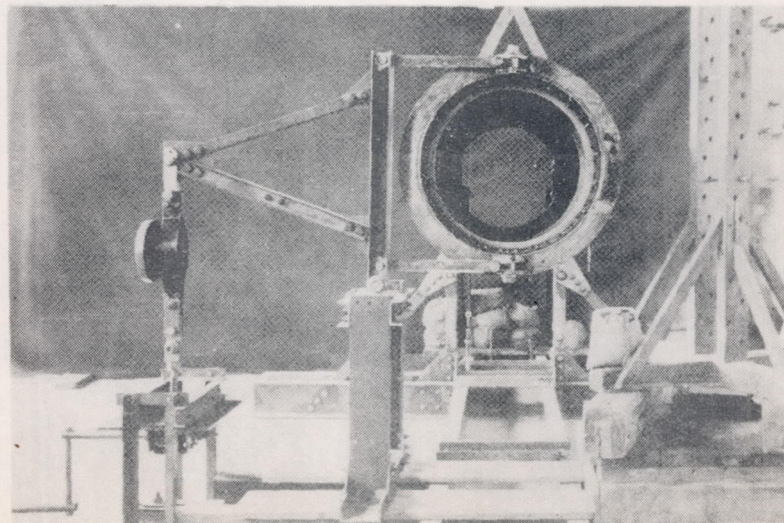
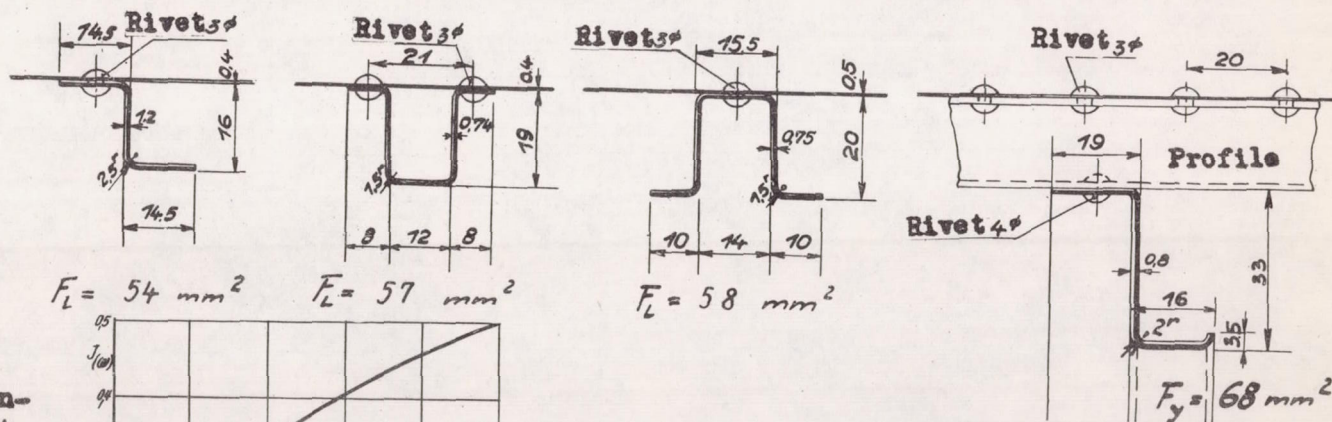
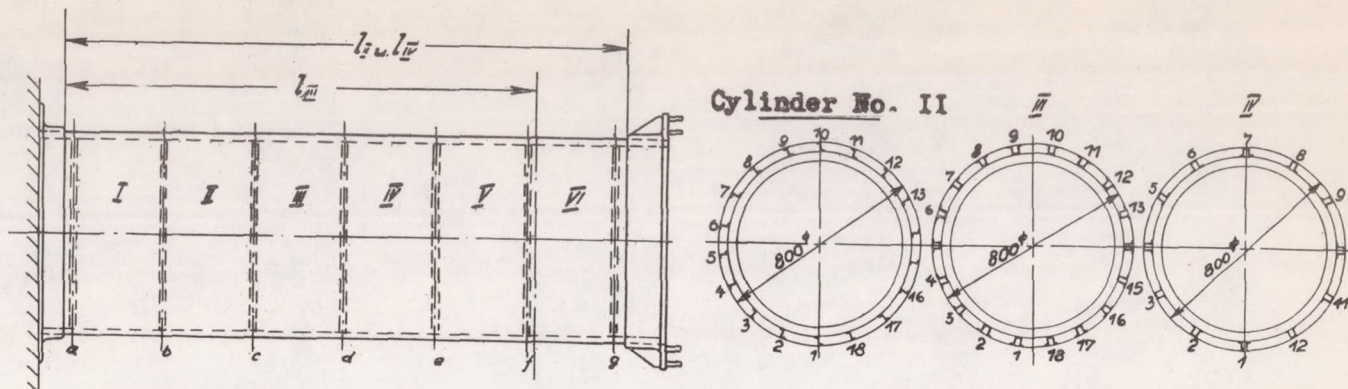


Figure 12.- Experimental setup for twisting tests.



$F_L = 54 \text{ mm}^2$        $F_L = 57 \text{ mm}^2$

$F_L = 58 \text{ mm}^2$

$F_y = 68 \text{ mm}^2$

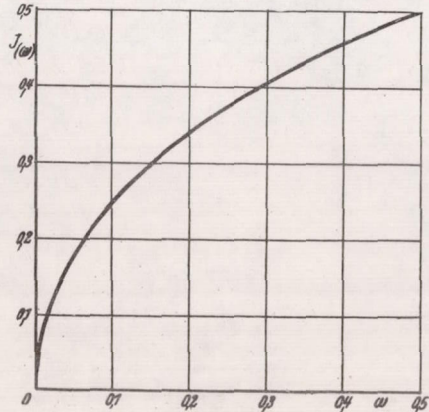


Figure 10.- Curve of integral

$$J(\omega) = \frac{2}{\pi} \int_0^{\pi/2} \sin \frac{1}{\omega} x dx.$$

Figure 11.-  
Schematic presentation of the test specimens.

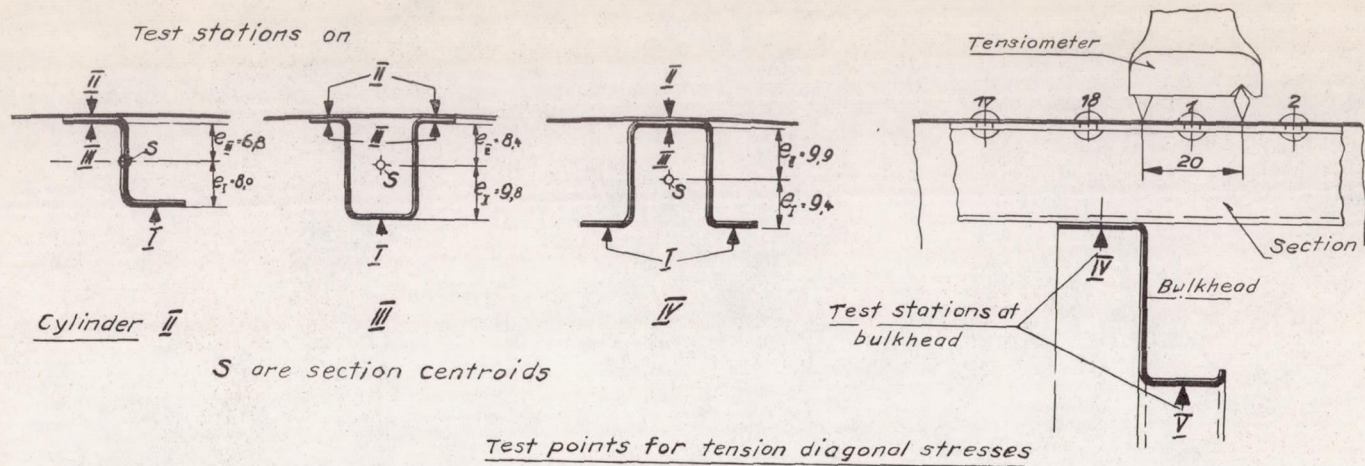


Figure 13.- Summary of test stations.

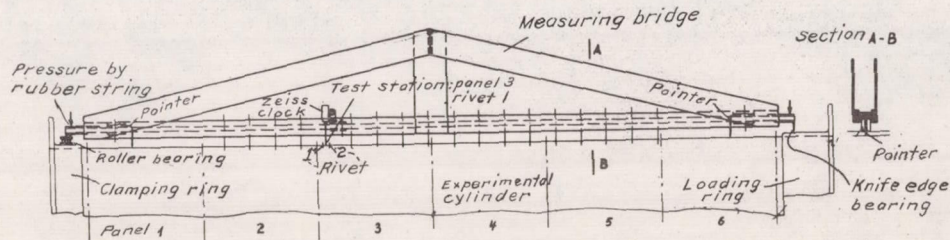


Figure 14.- Mechanical bridge.

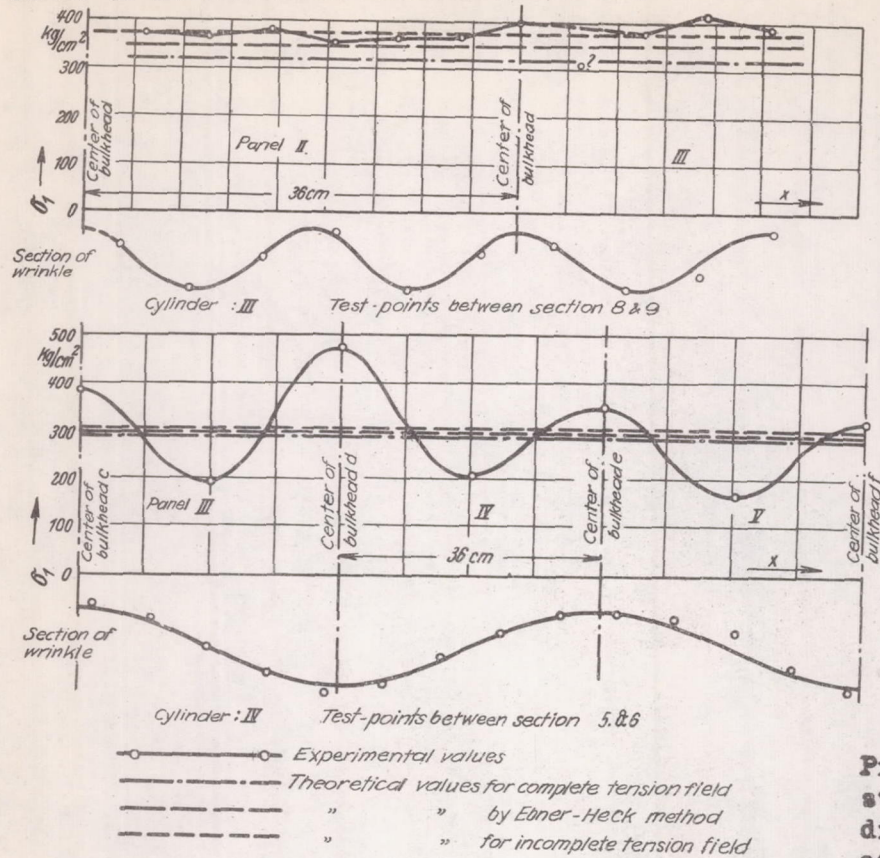


Figure 15.-  
Principal tensile stress  $\sigma_1$  (tension diagonal stress) at panel center.

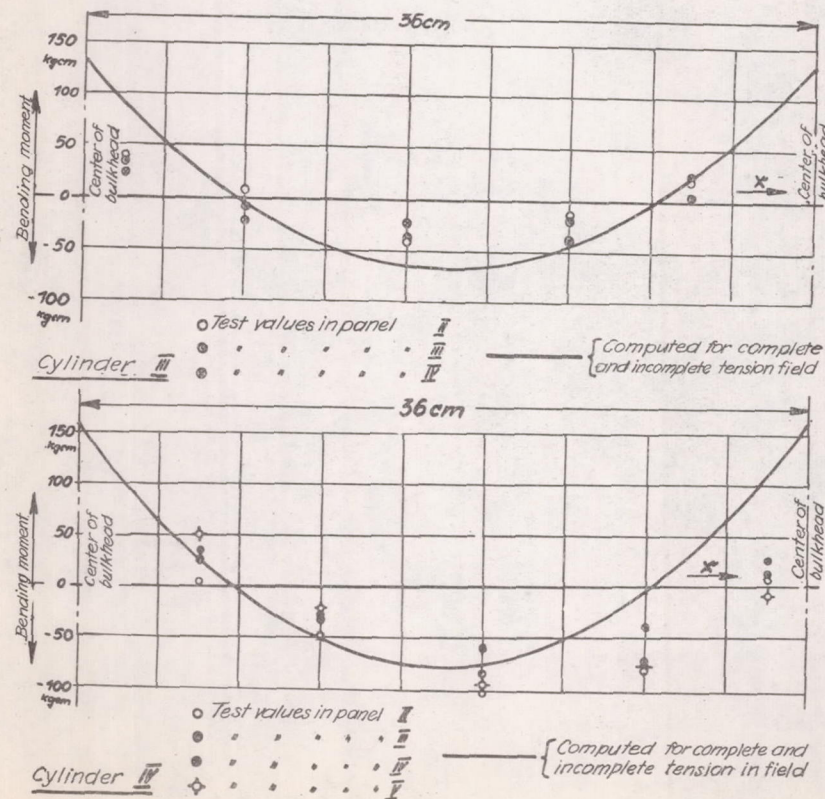
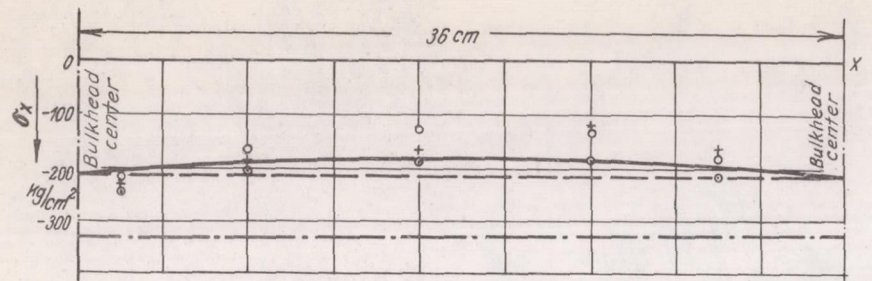
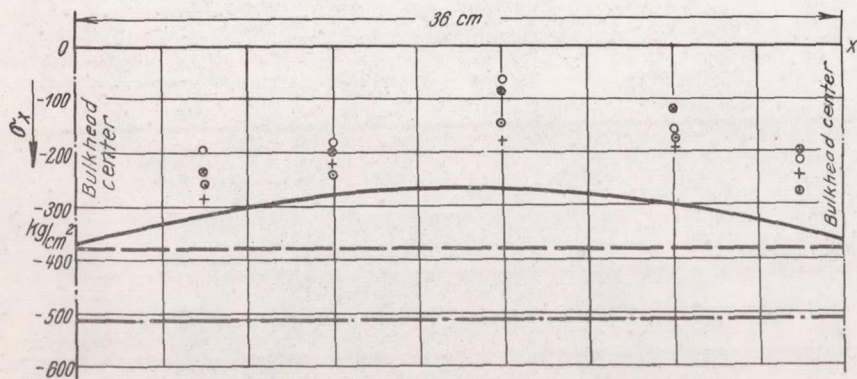


Figure 16.-  
Bending moment curves (theoretical and experimental) of the stringers.



Cylinder III {  $\circ$  Test points in panel II  
 + " " " " III  
 $\circ$  " " " " IV

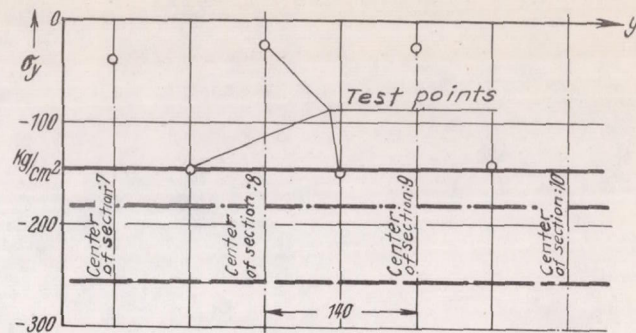
— — — — Computed for complete tension field  
 - - - - " " incomplete " "  
 - · - · - " " (Ebner - Heck method)



Cylinder IV {  $\circ$  Test points in panel II  
 + " " " " III  
 $\circ$  " " " " IV

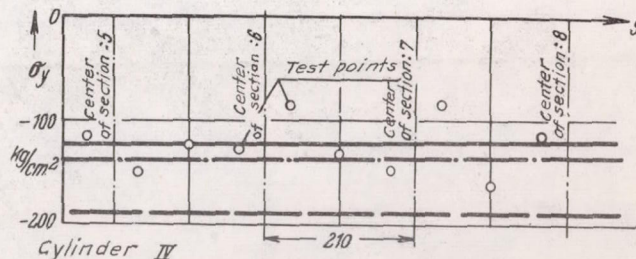
— — — — Computed for complete tension field  
 - - - - " " incomplete " "  
 - · - · - " " (Ebner - Heck method)

Figure 17.- Compressive stresses  $\sigma_x$  in the stringers.



cylinder III

— — — — Experimental value  
 - - - - Theoretical value complete and incomplete tension field.  
 - · - · - Theoretical value (Ebner - Heck method)



Cylinder IV

— — — — Mean value from experiments  
 - - - - Theoretical value complete and incomplete tension field.  
 - · - · - Theoretical value (Ebner - Heck method)

Figure 18.- Compressive stresses  $\sigma_y$  in the bulkheads.

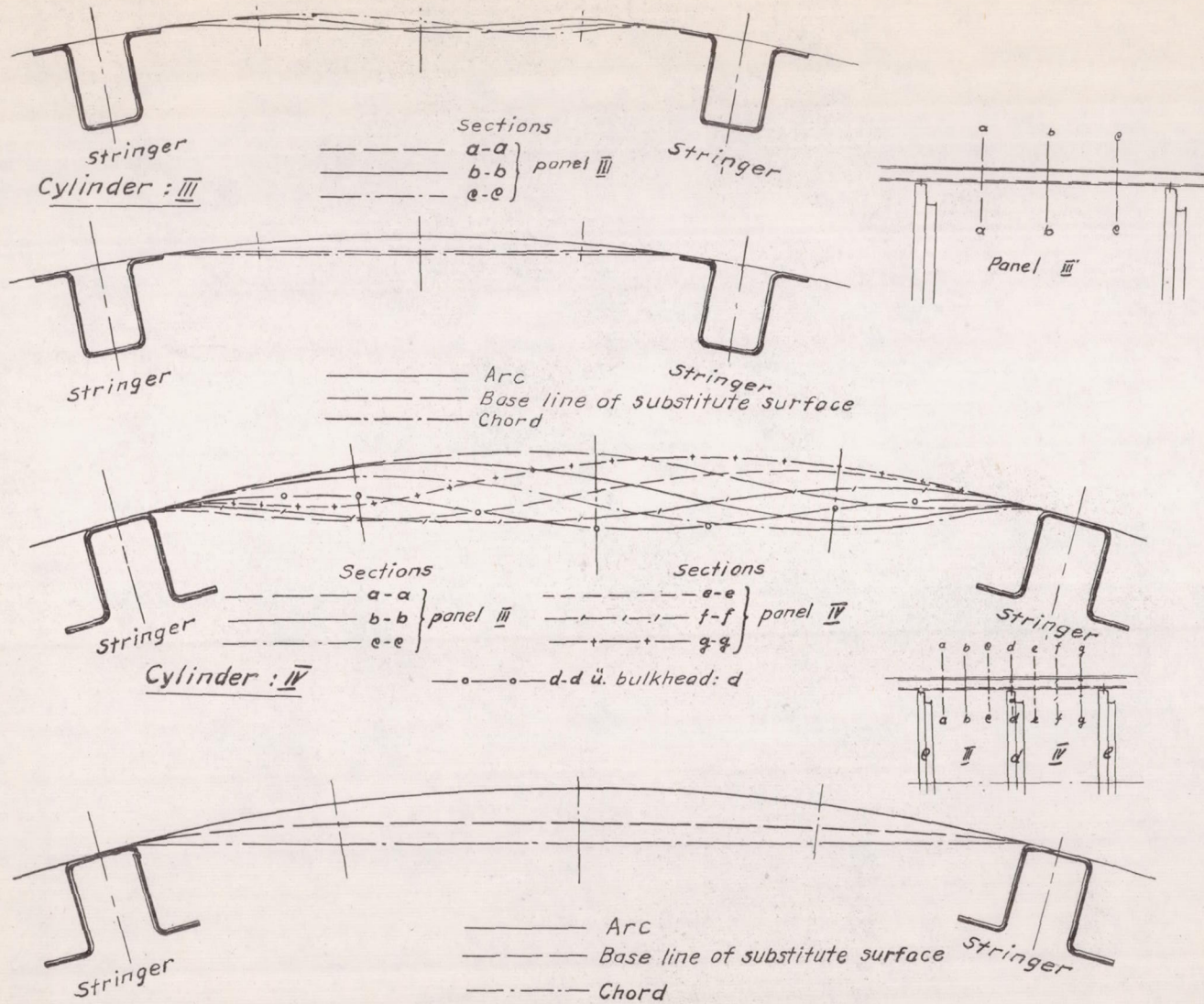


Figure 19.- Cross sections of buckling patterns.

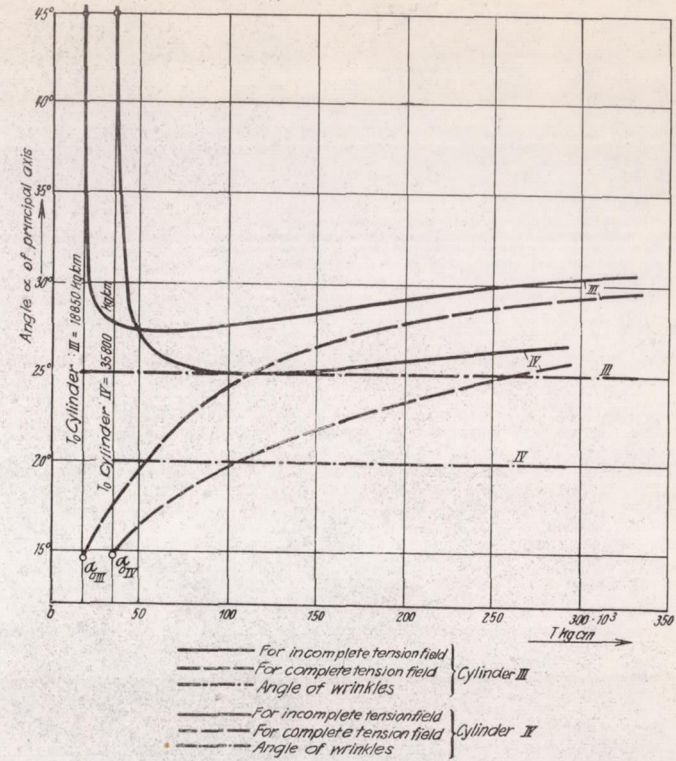
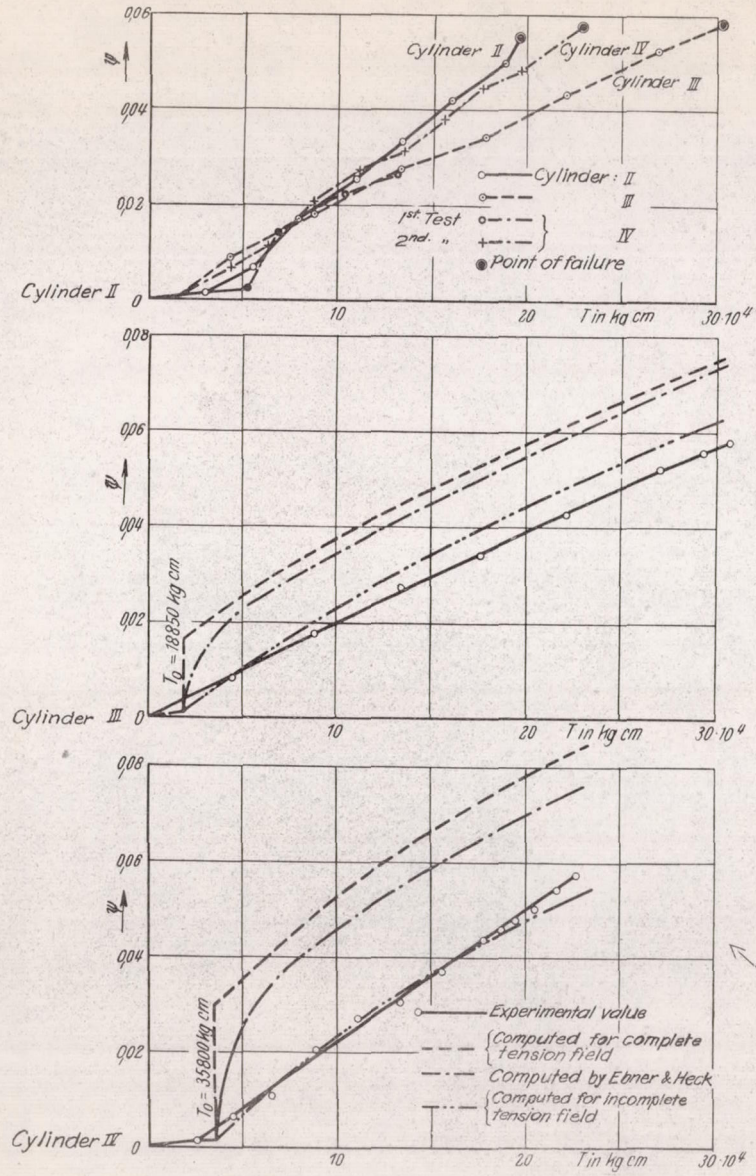


Figure 21.- Angle  $\alpha$  of the principal axes.

Figure 20.- Experimental and theoretical angle of twist  $\psi$ .

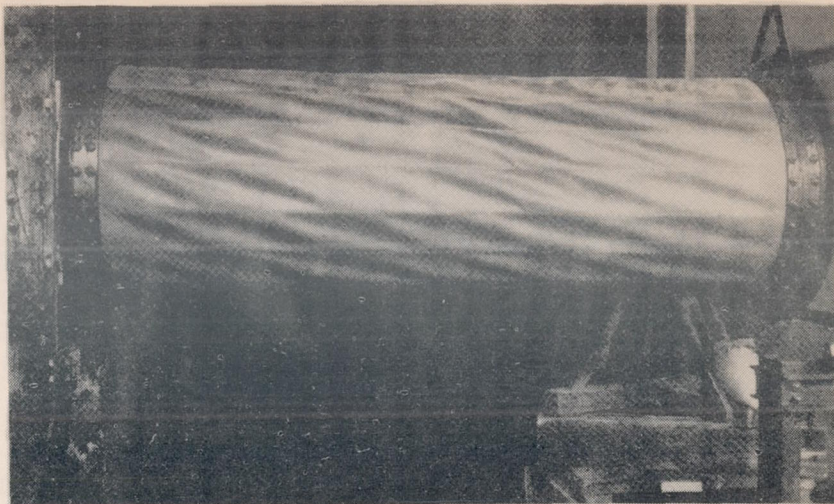
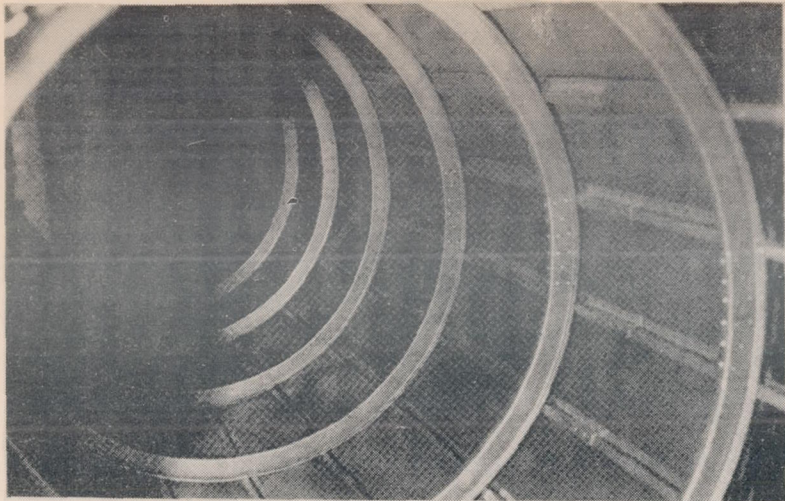


Figure 22.- Failure of cylinder No. II in pure twist. (inside view) Figure 23.- Failure of cylinder No. II in pure twist. (outside view)

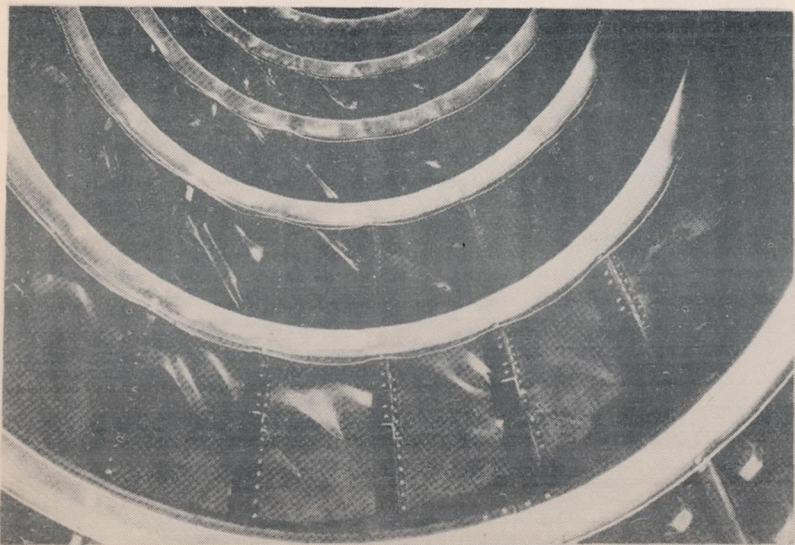


Figure 24.- Failure of cylinder No. III in pure twist (inside view).

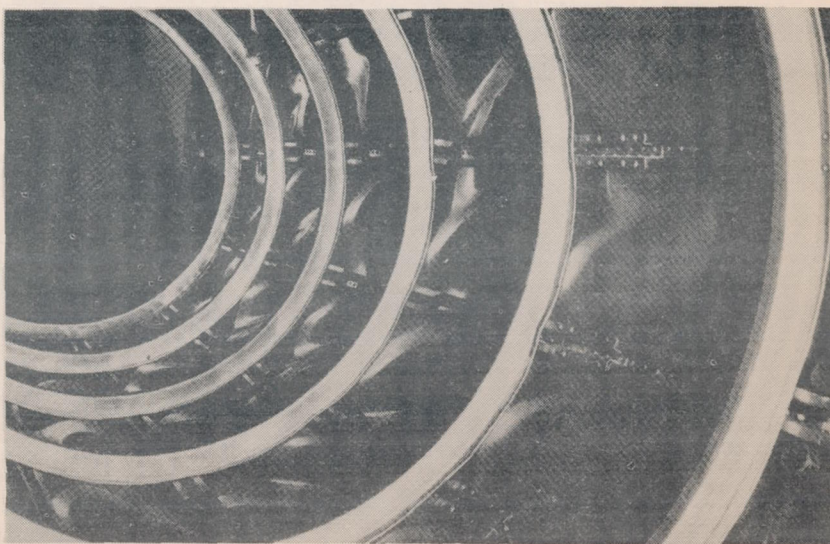


Figure 25.- Failure of cylinder No. IV in pure twist (inside view).

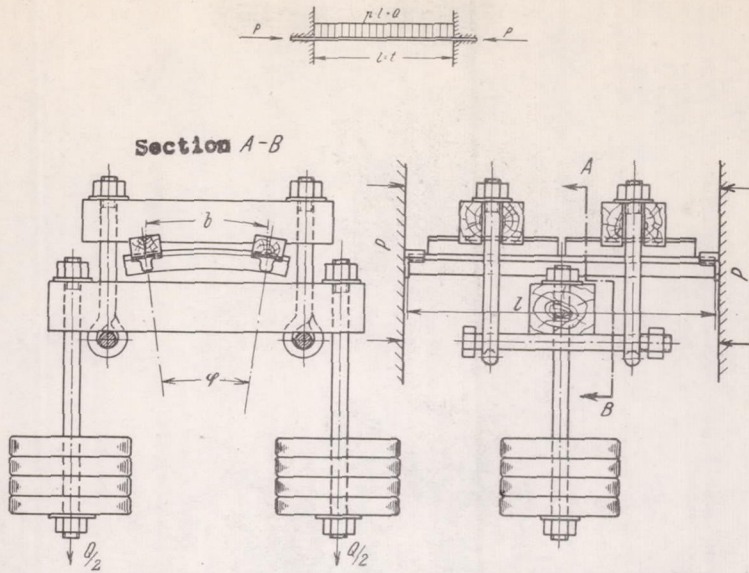


Figure 26.- Loading system and test arrangement for buckling-bending test with steel panels.

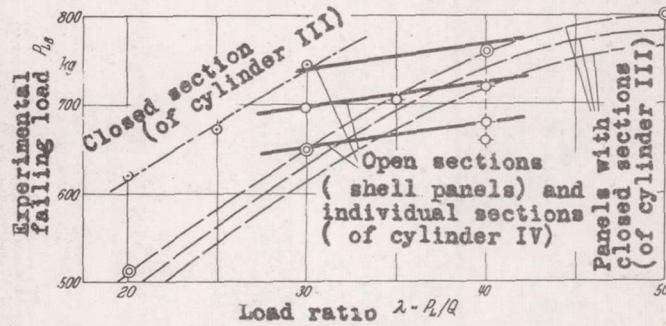


Figure 27.- Stringer failing loads  $P_s$  against load ratio  $\lambda$ .

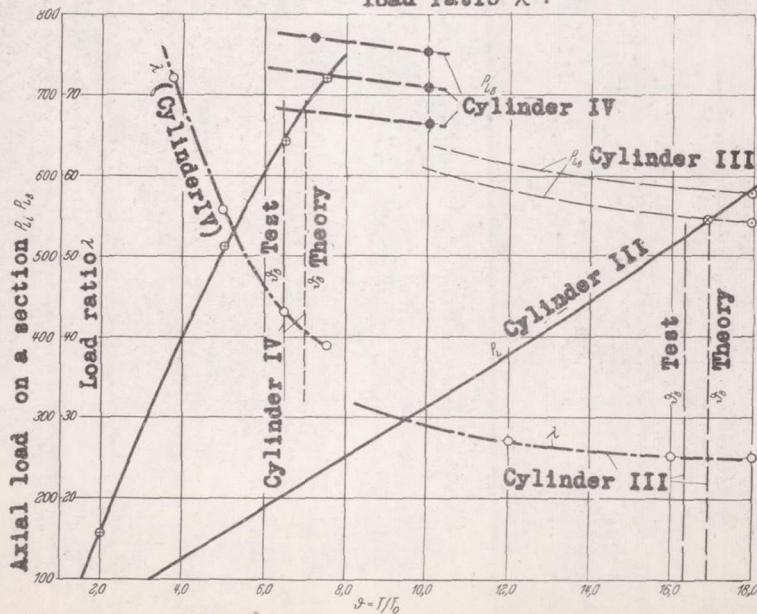


Figure 28.- Load ratio  $\lambda$ , axial load  $P_L$  and stringer capacity  $P_{LB}$  plotted against  $\phi = T/T_0$ .